Supporting Information

The ‘π-Trap’ as an Unrestricted Crystal Sponge for Inherently Amorphous Cluster Compounds

Yaofeng Wang[1], Niklas Rinn[1], Kevin Eberheim[2], Ferdinand Ziese[2], Jan Christmann[1], Simone Sanna[2], and Stefanie Dehnen[1,*]

([1]) Karlsruhe Institute of Technology, Institute of Nanotechnology. Kaiserstrasse 12, 76131 Karslruhe, Germany

([2]) Institut für Theoretische Physik and Center for Materials Research (LaMa), Justus-Liebig-Universität Gießen, 35392 Gießen, Germany

*Corresponding author(s). E-mail(s): stefanie.dehnen@kit.edu;

Contents

1. Supplementary Information of the X-ray Diffraction Analyses of Single Crystalline Compounds 1 – 3

Supplementary Table 1 | Crystallographic data and details of the structure determinations of compound 1 – 3.

Compound	$[(PhSn)_4S_6]_2\cdot(C_{60})\cdot(C_7H_8)_{1.2}\cdot(C_4H_8O)_{1.2}$ (**1**)	$[(PhSn)_4S_6]_2\cdot(C_{60})_{1.5}\cdot(C_7H_8)$ (**2**)	$[(PhSn)_4Se_6]\cdot(C_{60})\cdot(C_7H_8)\cdot(C_4H_8O)_{0.5}$ (**3**)
Chemical formula	$C_{121.2}H_{59.2}O_{1.2}S_{12}Sn_8$	$C_{145}H_{48}S_{12}Sn_8$	$C_{93}H_{32}O_{0.5}Se_6Sn_4$
Formula weight /[g mol^{-1}]	2868.72	3124.07	2105.70
Temperature/K	150	150	180
Crystal system	monoclinic	monoclinic	orthorhombic
Space group	$R\bar{3}$	$P2_1/c$	*Pbnb*
a/Å	27.2073(14)	23.032(4)	18.6432(11)
b/Å	27.2073(14)	19.248(3)	25.1311(15)
c/Å	35.229(2)	24.378(5)	28.9919(17)
α/°	90	90	90
β/°	90	102.013(15)	90
γ/°	120	90	90
Volume/Å^3	22584(3)	10565.5(15)	13583.4(14)
Z	9	4	8
ρ_{calc}g/cm3	1.898	1.964	2.059
μ/mm-1	12.306	11.895	10.626
F(000)	12492.0	6040.0	7984.0
Crystal size/mm^3	0.2 × 0.15 × 0.1	0.06 × 0.04 × 0.02	0.1 × 0.1 × 0.05
Radiation	Ga/Kα ($\lambda = 1.34143$)	Ga/Kα ($\lambda = 1.34143$)	GaKα ($\lambda = 1.34143$)
2Θ range for data collection/°	3.926 to 104.996	5.136 to 111.766	5.78 to 111.432
Index ranges	$-32 \leq h \leq 32$, $-23 \leq k \leq 32$, $-41 \leq l \leq 39$	$27 \leq h \leq 28$, $-23 \leq k \leq 21$, $-29 \leq l \leq 19$	$-18 \leq h \leq 22$, $-28 \leq k \leq 30$, $-35 \leq l \leq 23$
Reflections collected	48201	63933	50996
Independent reflections	8688 [$R_{int} = 0.1291$, $R_{sigma} = 0.1095$]	19768 [$R_{int} = 0.0430$, $R_{sigma} = 0.0603$]	12910 [$R_{int} = 0.0709$, $R_{sigma} = 0.1413$]
Goodness-of-fit on F^2	1.056	1.026	0.716
Final R indexes [I ⩾ 2σ (I)]	$R_1 = 0.0757$, $wR_2 = 0.1937$	$R_1 = 0.0562$, $wR_2 = 0.1305$	$R_1 = 0.0308$, $wR_2 = 0.0499$
Final R indexes [all data]	$R_1 = 0.1155$, $wR_2 = 0.2046$	$R_1 = 0.1034$, $wR_2 = 0.1604$	$R_1 = 0.0774$, $wR_2 = 0.0533$
Largest diff. peak/hole / e Å^{-3}	1.41/-1.31	1.71/-1.92	0.97/-0.54
CCDC deposition number	2419991	2419992	2419993

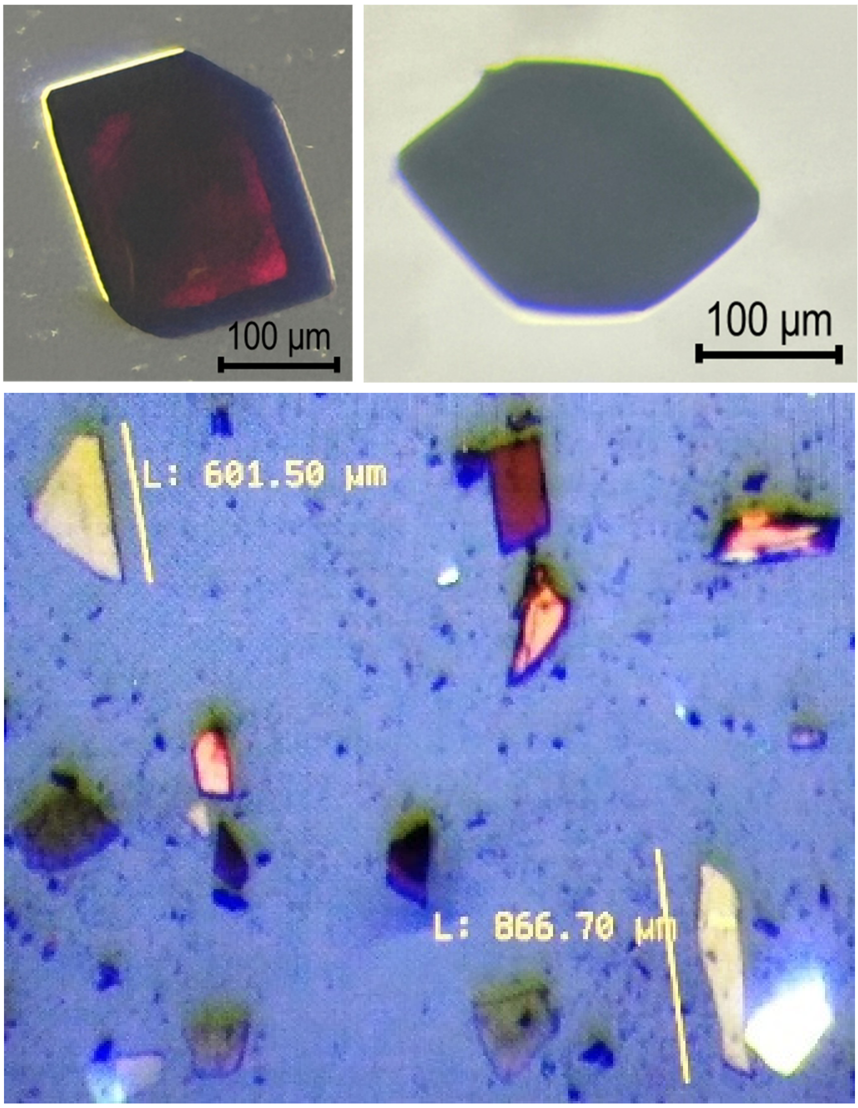

Supplementary Figure 1 | Optical photograph of crystals of compounds 1 (top left), 2 (top right), and 3 (bottom).

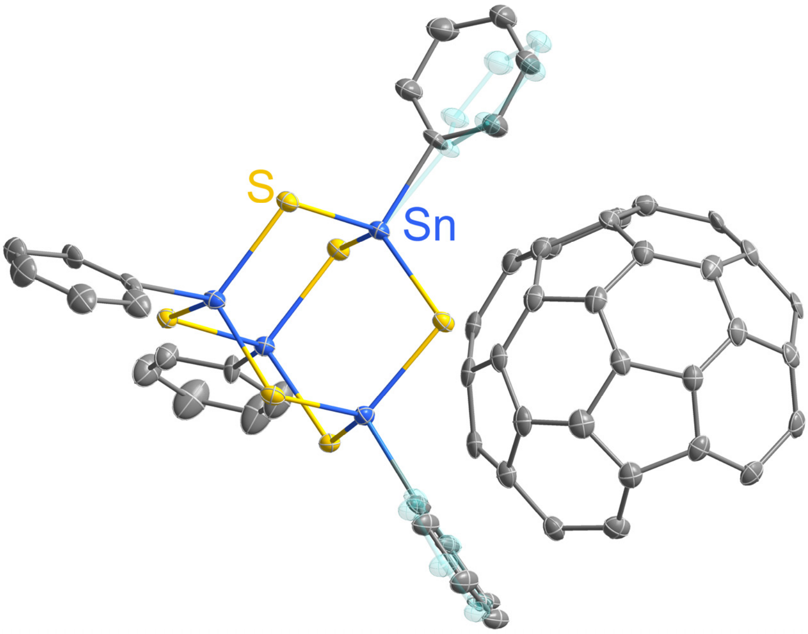

Supplementary Figure 2 | Asymmetric unit of the crystal structure of compound 1. Ellipsoids are shown at 30% probability. The disorder of the phenyl groups is shown as transparent atoms. H atoms are omitted for clarity.

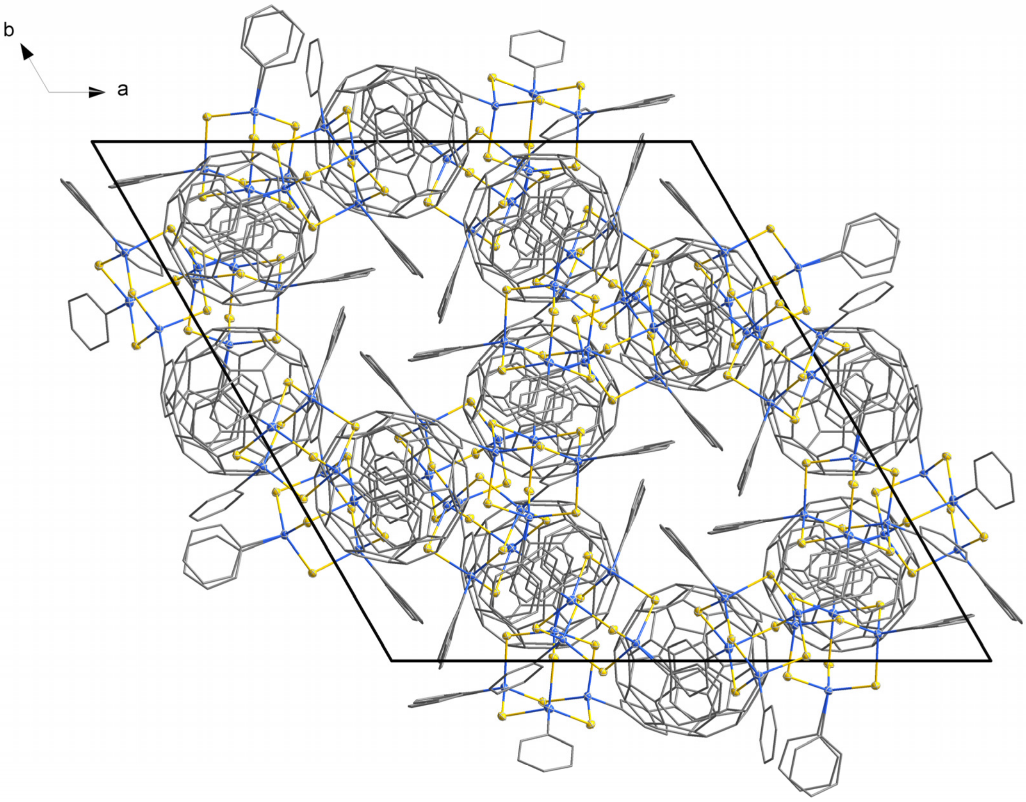

Supplementary Figure 3 | Extended unit cell of the crystal structure of 1 viewed along the crystallographic c-axis. Ellipsoids are shown at 30% probability. Solvent molecules were masked with the Olex2 mask function and H atoms are omitted for clarity.

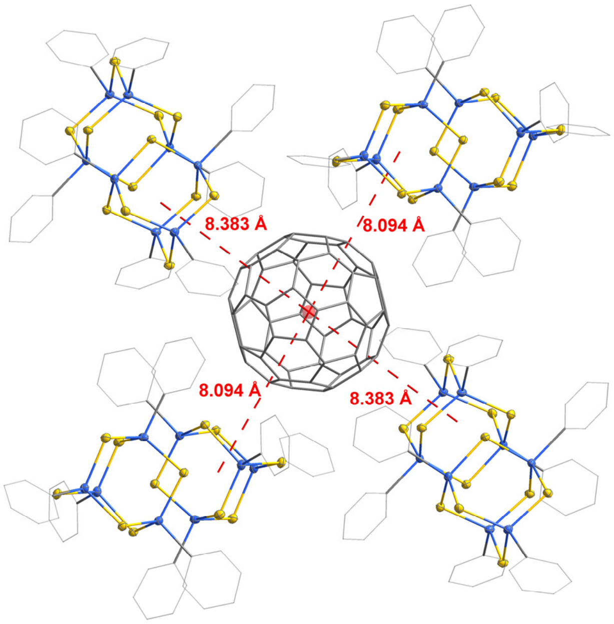

Supplementary Figure 4 | Cutout of the crystal structure of 1, showing the surrounding of each C_{60} molecule and their interaction with surrounding [$(PhSn)_4S_6$] pairs. Ellipsoids are shown at 30% probability. The disorder of the phenyl groups is omitted for clarity, only the major component of the disordered parts is shown.

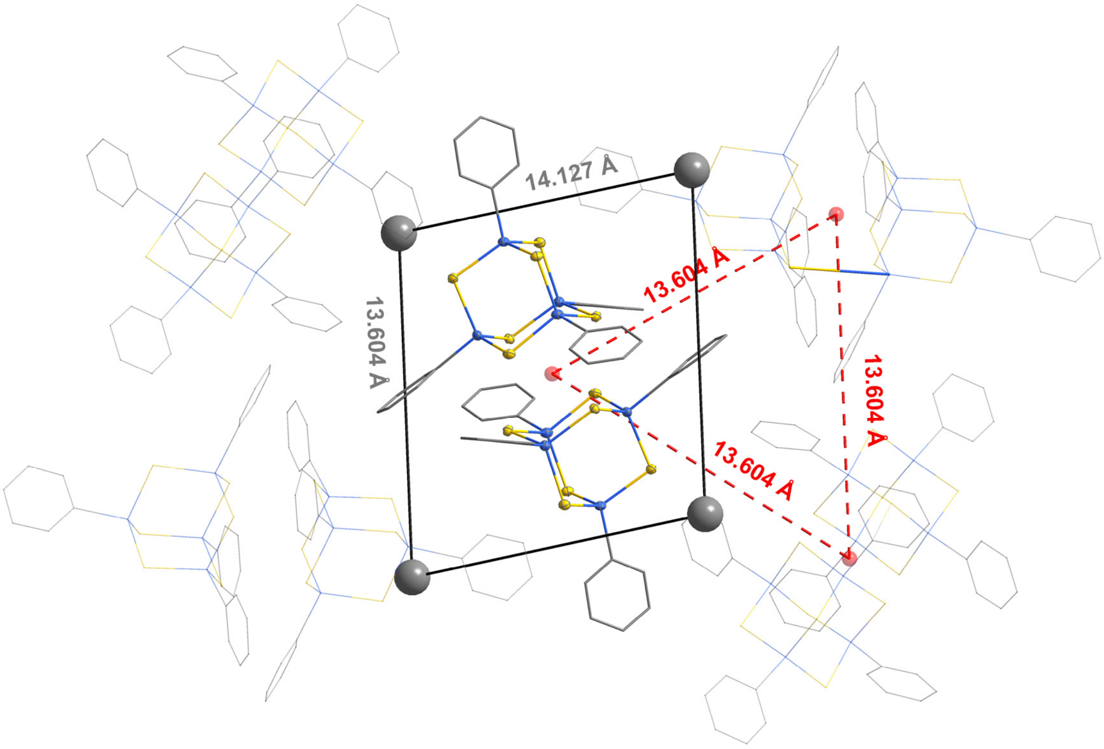

Supplementary Figure 5 | The [$(PhSn)_4S_6$] pair in the crystal structure of compound 1. The figure illustrates the interaction of [$(PhSn)_4S_6$] molecules with surrounding C_{60} molecules (here simplified as their centroids as grey spheres) and adjacent [$(PhSn)_4S]_6$ pairs. Ellipsoids are shown at 30% probability.

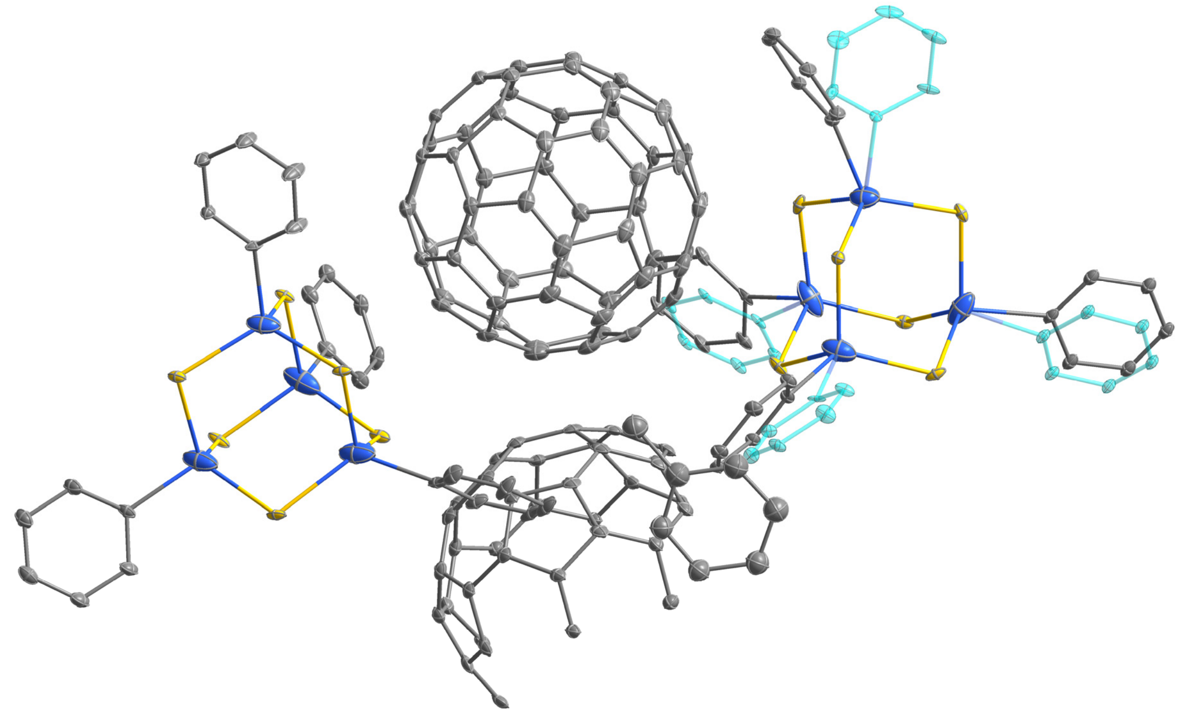

Supplementary Figure 6 | Asymmetric unit of the crystal structure of 2. Ellipsoids are shown at 30% probability. The disorder in the positions of the phenyl groups is shown as transparent atoms. H atoms are omitted for clarity.

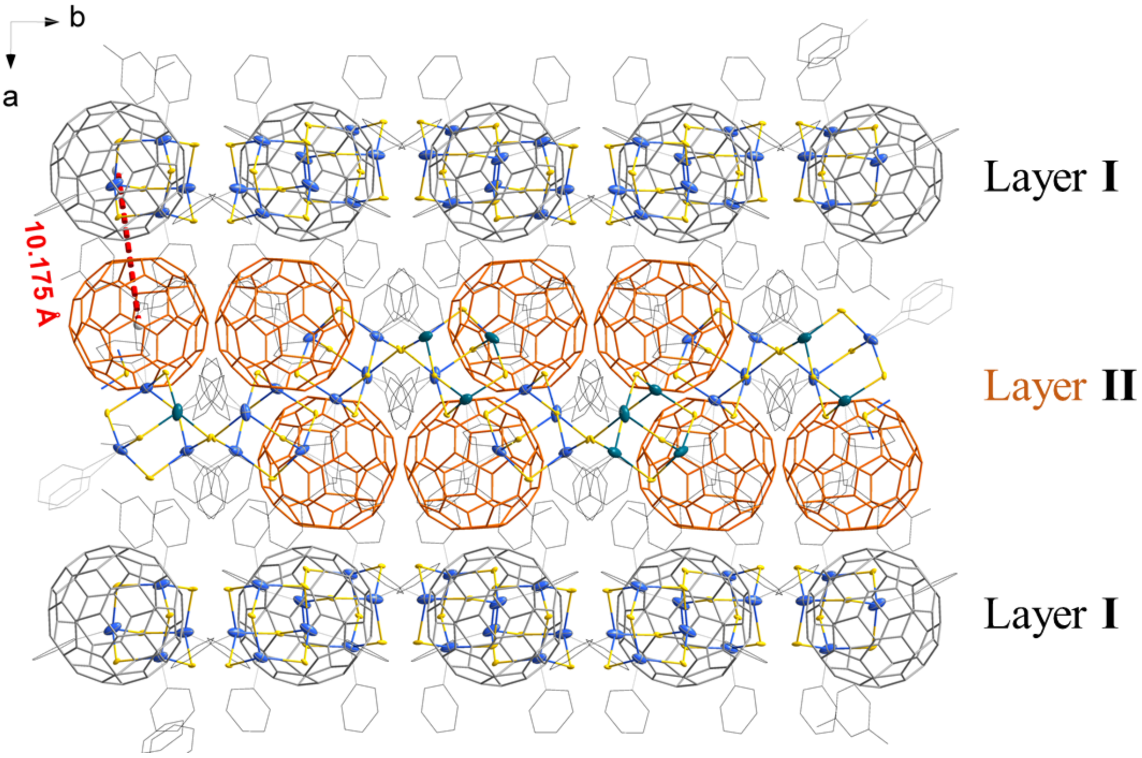

Supplementary Figure 7 | Packing of the molecules in 2 viewed along the crystallographic c-axis. Ellipsoids are shown at 30% probability. Hydrogen atoms are omitted for clarity.

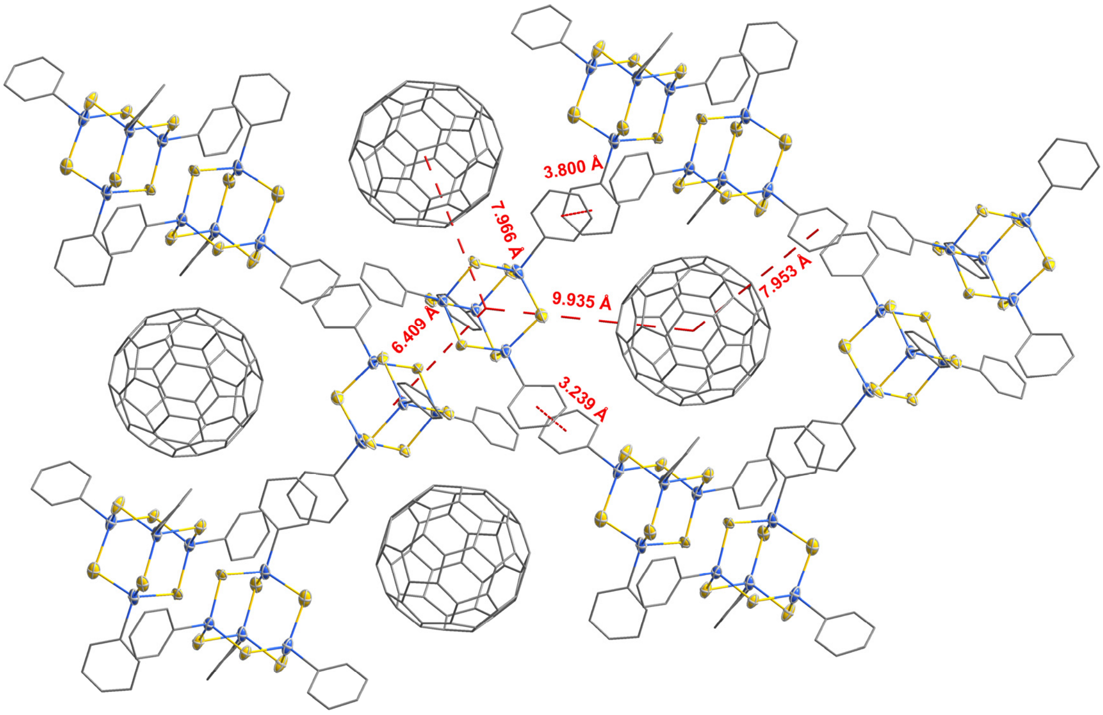

Supplementary Figure 8 | Packing of the molecules in layer I of the crystal structure of compound 2 viewed along the crystallographic a-axis. Ellipsoids are shown at 30% probability.

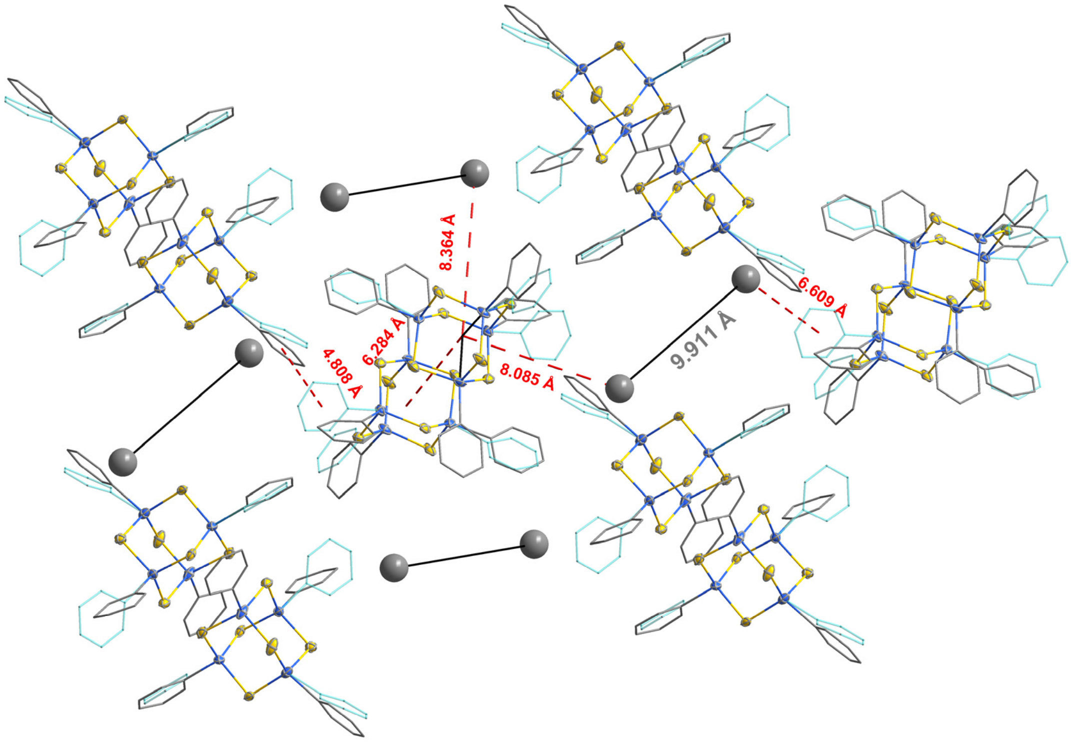

Supplementary Figure 9 | Packing of the molecules in layer II of the crystal structure of compound 2 viewed along the crystallographic a-axis. C_{60}s are only shown as grey spheres at their centroid positions. Ellipsoids are shown at 30% probability.

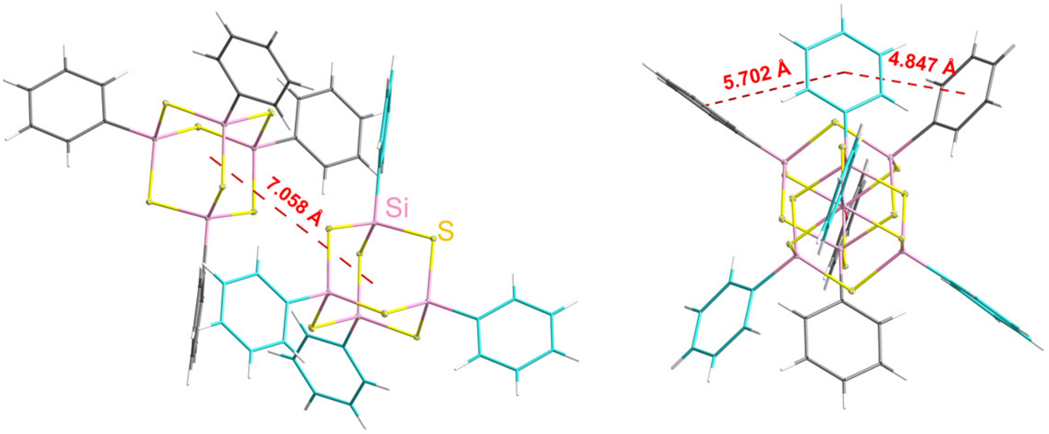

Supplementary Figure 10 | Cluster pair in the crystal structure of [(PhSi)$_4$S$_6$] (C)[1] (two views) for comparison. Ellipsoids are shown at 30% probability. The phenyl groups are depicted in grey and teal for the two distinct [(PhSi)$_4$S$_6$] molecules within the pair, respectively.

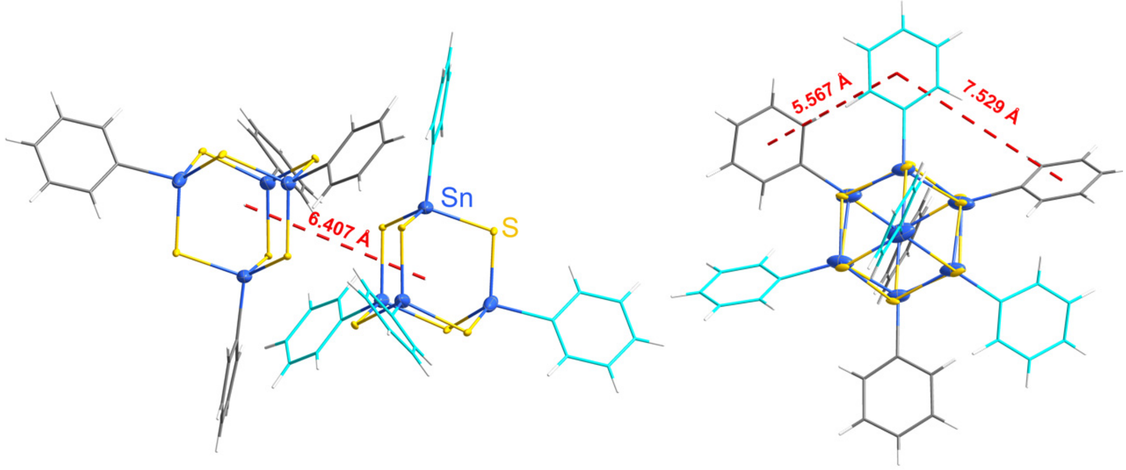

Supplementary Figure 11 | Orientation of the [(PhSn)$_4$S$_6$] pair in layer I of the crystal structure of 2 (two views). Ellipsoids are shown at 30% probability. The phenyl groups are depicted in grey and teal for the two distinct [(PhSn)$_4$S$_6$] molecules within the pair, respectively.

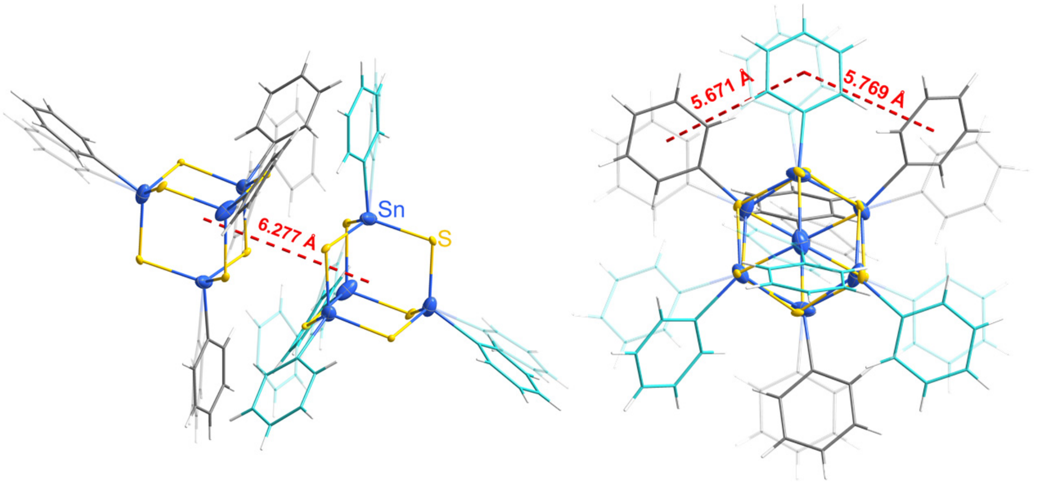

Supplementary Figure 12 | The orientation of the [(PhSn)$_4$S$_6$] pairs in layer II of the crystal structure of 2 (two views). The phenyl groups are depicted in grey and teal for the two distinct [(PhSn)$_4$S$_6$] molecules within the pair, respectively. Ellipsoids are shown at 30% probability.

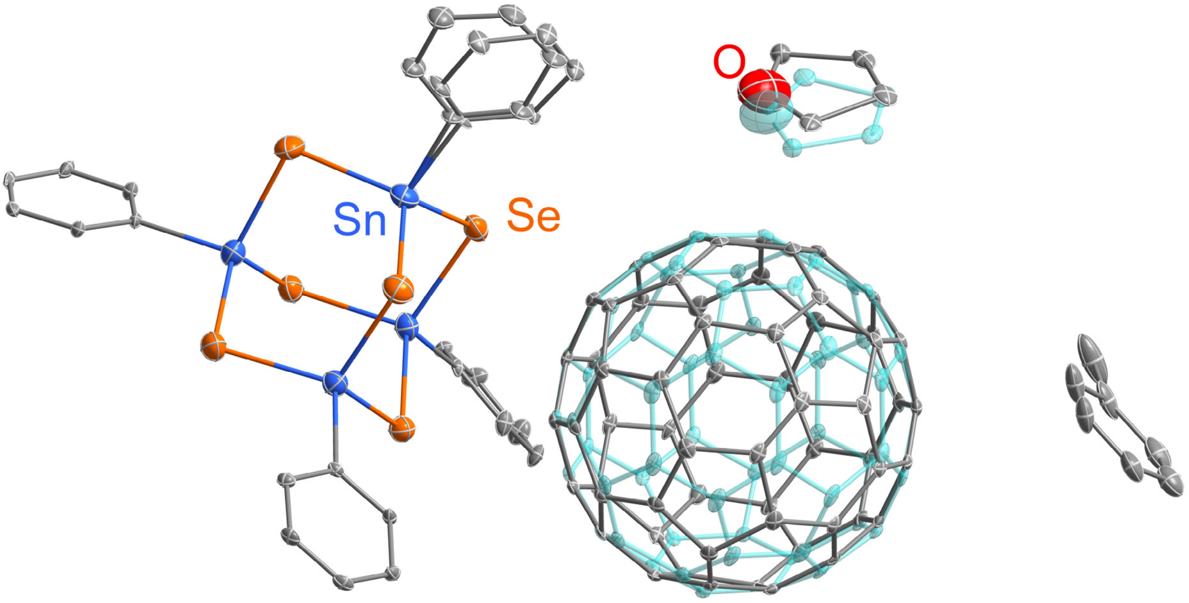

Supplementary Figure 13 | Asymmetric unit of the crystal structure of 3. Ellipsoids are shown at 30% probability. The disorder of the phenyl groups is shown as transparent atoms. H atoms are omitted for clarity.

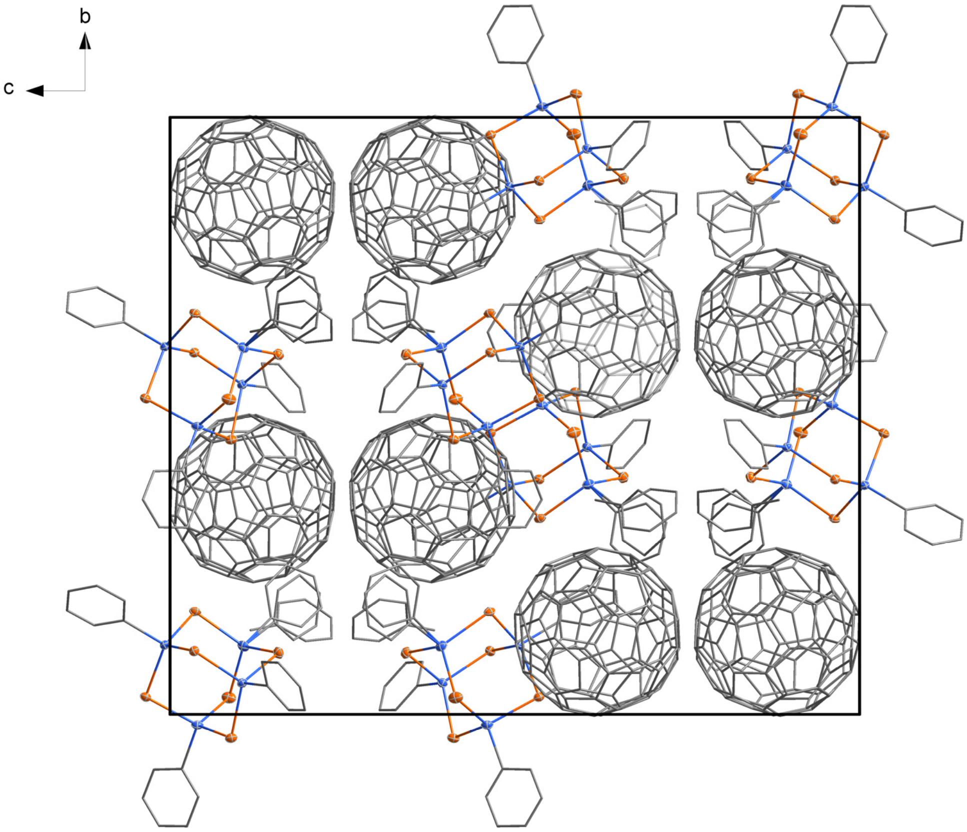

Supplementary Figure 14 | Extended unit cell of the crystal structure of 3 viewed along the crystallographic a-axis. Ellipsoids are shown at 30% probability. Solvents are masked with Olex2 mask function and H atoms are omitted for clarity.

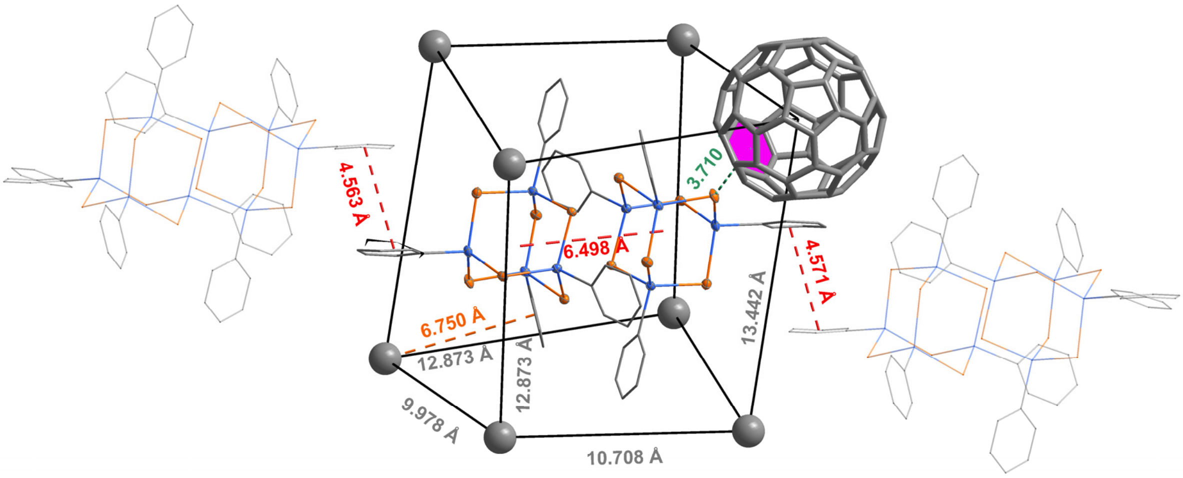

Supplementary Figure 15 | Cutout from the structure of 3. The figure illustrates the interactions of [(PhSn)$_4$Se$_6$] molecules with surrounding C$_{60}$ molecules (here simplified as their centroids as grey spheres) and adjacent [(PhSn)$_4$Se$_6$] pairs. Ellipsoids are shown at 30% probability.

Supplementary Table 2 | Selected bonds length and angles of [(PhSn)$_4$S$_6$] in compounds 1 and 2, [(PhSn)$_4$Se$_6$] in compound 3, and [(PhSi)$_4$S$_6$] in compound C[1] for comparison.

Compound	Bond distance / Angle	
[(PhSn)$_4$S$_6$] in **1**	Sn–S	2.395(4) – 2.411(3) Å
	Sn–C	2.103(14) –2.120(17) Å
	Sn…Sn	3.7631(13) –3.8105(18) Å
	S…S	3.9139(48) – 3.9727(60) Å
	S–Sn–S	108.95(13) – 116.00(12) °
	Sn–S–Sn	103.49(13) –105.31(13) °
[(PhSn)$_4$S$_6$] in **2**	Sn–S	2.38(1) –2.411(9) Å
	Sn–C	2.105(12) –2.166(17) Å
	Sn…Sn	3.7427(12) –3.8287(12) Å
	S…S	3.8753(44) – 4.0789(44) Å
	S–Sn–S	107.8(4) – 116.0(3) °
	Sn–S–Sn	103.09(13) – 104.76(15) °
[(PhSn)$_4$Se$_6$] in **3**	Sn–Se	2.5135(7) –2.5337(7) Å
	Sn–C	2.11(2) –2.126(19) Å
	Sn…Sn	3.8952(20) – 3.9242(10) Å
	S…S	4.1581(37) –4.2870(39) Å
	Se–Sn–Se	110.50(2) – 116.24(2) °
	Sn–S–Sn	100.81(8) – 102.36(8) °
[(PhSi)$_4$S$_6$] in **C** (ref 1)	Si–S	2.1184(5) – 2.1476(5) Å
	Si–C	1.8540(15) –1.8562(15) Å
	Si…Si	3..3393(5) – 3.3676(6) Å
	S…S	3.5237(5) – 3.5638(5) Å
	S–Si–S	111.29(2) – 113.27(2) °
	S–S–Si	103.22(2) – 104.25(2) °

2. First-principles calculations of the electronic properties of the co-crystals

Supplementary Table 3 | Lattice parameters of the crystalline compounds 1, 2 and 3 as calculated within DFT.

	Crystal lattice type	**a [Å]**	**b [Å]**	**c [Å]**	$\boldsymbol{\alpha}$	$\boldsymbol{\beta}$	$\boldsymbol{\gamma}$
1	Hexagonal	27.207	27.207	35.229	90°	90°	120°
2	Monoclinic	23.032	19.248	24.378	90°	90°	102.013°
3	Orthorhombic	18.643	25.131	28.992	90°	90°	90°

The core center-to-center distances as well as the shortest distances between chalcogenide atoms (S or Se) and the hexagonal faces of neighboring C_{60} molecules are within 1% of the measured values.

In order to estimate the extension of the cluster core, a convex hull's volume of the core is considered. The corresponding results are shown in **Supplementary Table 4**, which demonstrates that the core volume is substantially preserved upon crystallization. The volume of **C**, reported for comparison, is substantially smaller. **Supplementary Table 4** also shows the Si–S, Sn–S as well as Sn–Se bond lengths of the investigated compounds. The average bond length roughly mirrors the sum of the covalent radii of the involved atoms. The difference between maximal and minimal bond length is a measure for the deviation from the ideal tetragonal symmetry of the adamantane-based core, and can thus be interpreted as a core distortion. We observe that the deviation from the tetragonal symmetry is similar in **A**, **B** and **C**. Upon crystallization, the core distortion is enhanced, in particular for crystal **3** containing Se.

Supplementary Table 4 | Core volume and T–E bond lengths as calculated by DFT for the investigated compounds. Minimal, maximal and average bond lengths are given, as well as the difference between smallest and largest length. The latter is a measure for the core distortion. All lengths are given in Å, volumes in Å^3.

	Core volume	Min.	Max.	Avg.	Diff.
C [$(PhSi)_4S_6$]	25.83	2.140	2.153	2.15	0.013
A [$(PhSn)_4S_6$]	37.46	2.424	2.436	2.43	0.012
B [$(PhSn)_4Se_6$]	44.03	2.554	2.565	2.56	0.011
1	37.26	2.421	2.440	2.43	0.019
2	37.29	2.420	2.444	2.43	0.024
3	43.94	2.534	2.578	2.56	0.044

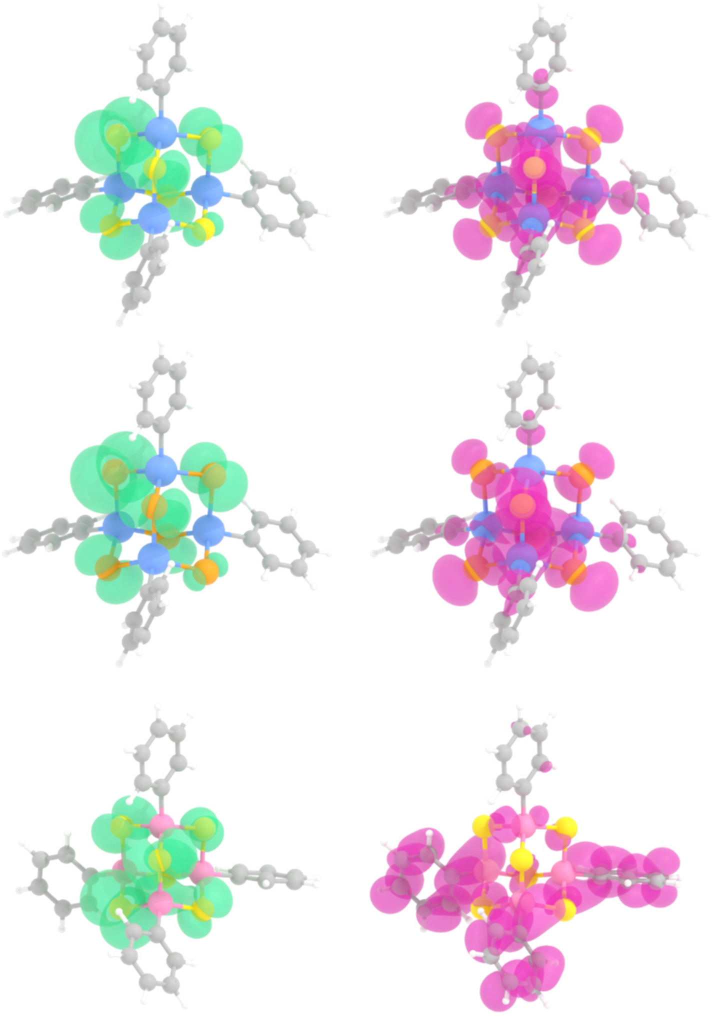

Supplementary Figure 16 | HOMO (left) and LUMO (right) of cluster [(PhSn)4S6] (A, top), $[(PhSn)_4Se_6]$ (B, center), and $[(PhSi)_4S_6]$ (C, center), calculated within DFT-PBE. The HOMO is strongly localized at the S atoms, while the LUMO is less localized at the S atoms and extends to the substituents. The isosurface at 0.001 e^{-3} is shown.

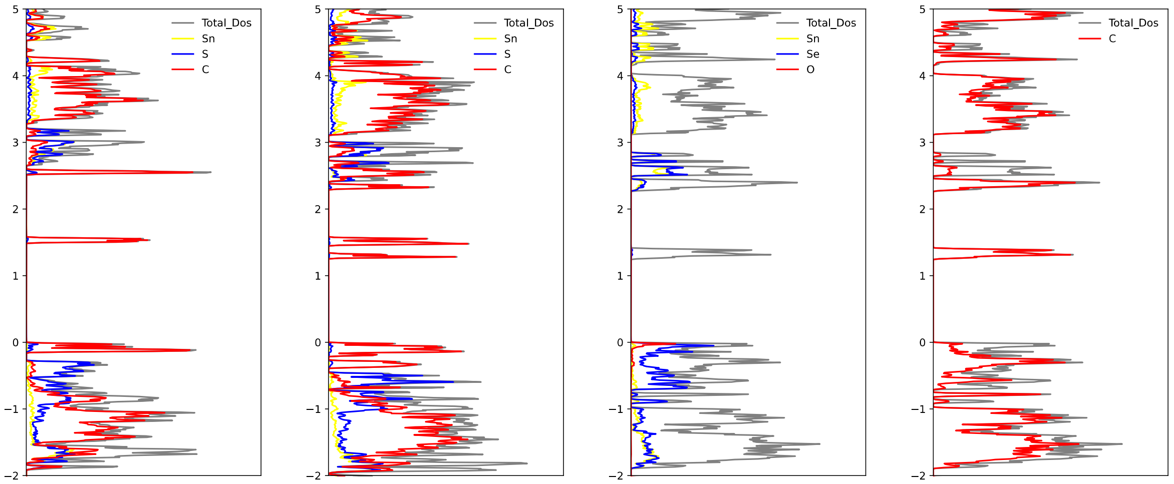

Supplementary Figure 17 | Density of states and partial density of states calculated within DFT-PBE for compounds 2 and 3. For the sake of clarity, the DOS of **3** is split into the last two panels. The corresponding graphic for compound **1** is given in **Figure 6f** in the main document.

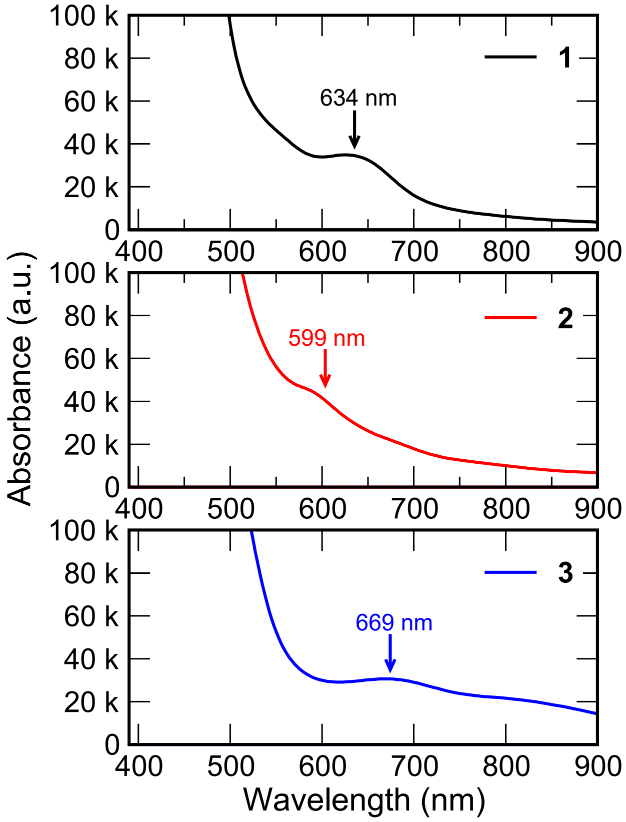

Supplementary Figure 18 | Optical absorption of 1, 2, and 3. Absorption coefficient of **1**, **2**, and **3** calculated in the independent particle approximation. The arrows mark spectral signatures related to electronic transitions involving the C_{60} states.

3. References

1. Rosemann, N. W., Eußner, J. P., Dornsiepen, E., Chatterjee, S. & Dehnen, S. Organotetrel Chalcogenide Clusters: Between Strong Second-Harmonic and White-Light Continuum Generation. *J. Am. Chem. Soc.* **138**, 16224–16227 (2016).